Stem Cell Reports
Article

ISSCR

OPEN ACCESS

Controlling the Regional Identity of hPSC-Derived Neurons to Uncover Neuronal Subtype Specificity of Neurological Disease Phenotypes

Kent Imaizumi,[1] Takefumi Sone,[1] Keiji Ibata,[1] Koki Fujimori,[1] Michisuke Yuzaki,[1] Wado Akamatsu,[1,2,*] and Hideyuki Okano[1,*]

[1]Department of Physiology, Keio University School of Medicine, 35 Shinanomachi, Shinjuku, Tokyo 160-8582, Japan
[2]Center for Genomic and Regenerative Medicine, Juntendo University School of Medicine, 2-1-1 Hongo, Bunkyoku, Tokyo 113-8421, Japan
*Correspondence: awado@juntendo.ac.jp (W.A.), hidokano@a2.keio.jp (H.O.)
http://dx.doi.org/10.1016/j.stemcr.2015.10.005

SUMMARY

The CNS contains many diverse neuronal subtypes, and most neurological diseases target specific subtypes. However, the mechanism of neuronal subtype specificity of disease phenotypes remains elusive. Although in vitro disease models employing human pluripotent stem cells (PSCs) have great potential to clarify the association of neuronal subtypes with disease, it is currently difficult to compare various PSC-derived subtypes. This is due to the limited number of subtypes whose induction is established, and different cultivation protocols for each subtype. Here, we report a culture system to control the regional identity of PSC-derived neurons along the anteroposterior (A-P) and dorsoventral (D-V) axes. This system was successfully used to obtain various neuronal subtypes based on the same protocol. Furthermore, we reproduced subtype-specific phenotypes of amyotrophic lateral sclerosis (ALS) and Alzheimer's disease (AD) by comparing the obtained subtypes. Therefore, our culture system provides new opportunities for modeling neurological diseases with PSCs.

INTRODUCTION

Modeling human diseases with pluripotent stem cells (PSCs), including embryonic stem cells (ESCs) and induced PSCs (iPSCs), has remarkable potential to generate new insights into understanding disease pathogenesis and to open up new avenues for effective therapies. In particular, modeling neurological diseases is of great interest given that it is difficult to obtain patient-derived neural cells or tissues because of the limited accessibility to the brain. Indeed, ESCs and iPSCs derived from patients have been used to study several neurological diseases, including amyotrophic lateral sclerosis (ALS; Dimos et al., 2008; Egawa et al., 2012), Alzheimer's disease (AD; Israel et al., 2012; Kondo et al., 2013; Yagi et al., 2011), Parkinson's disease (Devine et al., 2011; Imaizumi et al., 2012; Nguyen et al., 2011), schizophrenia (Brennand et al., 2011; Bundo et al., 2014; Hook et al., 2014), epilepsy (Higurashi et al., 2013; Jiao et al., 2013; Liu et al., 2013), and Rett syndrome (Andoh-Noda et al., 2015; Marchetto et al., 2010). Because most neurological diseases affect one or more specific lesion area(s), PSCs were differentiated into corresponding neuronal subtypes in such studies (Imaizumi and Okano, 2014; Marchetto and Gage, 2012; Mattis and Svendsen, 2011; Okano and Yamanaka, 2014). However, these approaches cannot procure the mechanism of subtype specificity of disease phenotypes; that is, why some neuronal subtypes are selectively damaged whereas others evade pathogenesis.

To clarify the mechanism of subtype specificity, it is necessary to compare phenotypes between disease-susceptible and -insusceptible neuronal subtypes. Nonetheless, this approach has not been developed to date for two reasons. First, only a few neuronal subtypes can be successfully induced from PSCs. Second, each previously reported protocol to induce specific subtypes varies in its cultivation procedures, giving rise to variability between protocols in efficiency, maturity, and culture-afflicted stress and preventing a direct comparison across different neuronal subtypes.

Here we addressed these problems by focusing on control of the regional identity of PSC-derived neural progenitors and neurons. The developing neural tube is subdivided into distinct regions along the anteroposterior (A-P) and dorsoventral (D-V) axes, and each region produces a specific subtype of neurons (Kiecker and Lumsden, 2012). Namely, neuronal subtype specification in the neural tube is determined in a region-specific manner. If the regional identity of PSC-derived neurons could be regulated at will based on the same protocol, then any desired subtypes could be induced with the same efficiency and under the same culture conditions. A protocol permitting such regulation would enable the reproduction of disease phenotypes in any given brain region and also the comparison of phenotypes between different neuronal subtypes.

In this study, we report a robust method to control the regional identity of PSC-derived neural progenitors and neurons based on a single protocol. To do so, Wnt, retinoic acid (RA), and sonic hedgehog (Shh) signaling were modulated to manipulate the A-P and D-V identities of neural progenitors. Regional identity was maintained throughout neural differentiation, generating a variety of neuronal

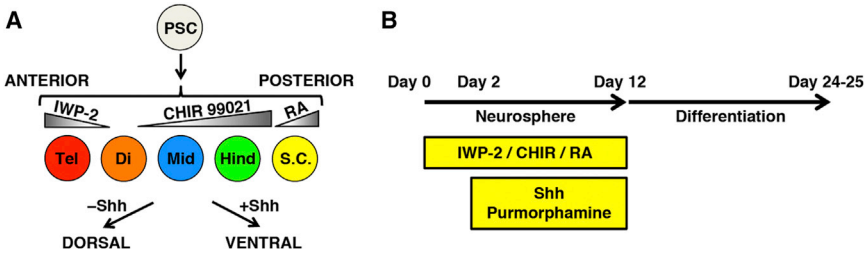

Figure 1. Strategy for Defining the Regional Identity of PSC-Derived Neural Progenitors

(A) Schematic of the strategy employed for the manipulation of regional identity. Wnt signaling was modulated by using the porcupine inhibitor IWP-2 and the GSK3β inhibitor CHIR. Tel, telencephalon; Di, diencephalon; Mid, midbrain; Hind, hindbrain; S.C., spinal cord.

(B) Overview of the culture protocol. Patterning factors (IWP-2, CHIR, RA, Shh, and purmorphamine) were added during neurosphere formation.

subtypes, including cortical projection neurons, cortical interneurons, midbrain dopaminergic neurons, hindbrain serotonergic neurons, spinal cord sensory interneurons, and spinal cord motor neurons. Finally, we compared these neuronal subtypes and detected ventral spinal cord-specific neurite swellings in ALS iPSCs and forebrain-specific accumulation of phosphorylated tau (p-tau) in AD iPSCs. Therefore, this culture system could be a useful tool to approach the mechanism of subtype specificity of neurological disease phenotypes.

RESULTS

Strategy for Defining the Regional Identity of PSC-Derived Neural Progenitors

Because Wnt, RA, and Shh signaling are involved in the formation of the A-P and D-V axes during neural development (Briscoe and Ericson, 2001; Marshall et al., 1992; Nordström et al., 2002), we explored the possibility that these patterning signaling molecules might have analogous effects in neural cells differentiated from PSCs. We hypothesized that the A-P identity (ranging from the telencephalon to the spinal cord) can be controlled by regulating Wnt and RA signaling and that the D-V identity can be controlled similarly by regulating Shh signaling (Figure 1A). To evaluate this hypothesis, we induced neural progenitors derived from ESCs (KhES-1; Suemori et al., 2006) by using the neurosphere culture system (modified from Chaddah et al., 2012) and treated the cells with modulators of these patterning signaling pathways during neurosphere formation (Figure 1B). The modulators included the porcupine inhibitor IWP-2 (a Wnt antagonist; Chen et al., 2009), the glycogen synthase kinase (GSK) 3β inhibitor CHIR99021 (a Wnt agonist, referred to hereafter as CHIR; Ring et al., 2003), RA, Shh protein, and the Smo receptor agonist purmorphamine (a Shh agonist; Sinha and Chen, 2006). Although the diameter of the neurospheres was increased by treatment with CHIR and RA, each of the experimental conditions was able to generate neurospheres (Figures S1A and S1B). Moreover, the patterning factors did not influence the number of neurospheres generated (Figure S1C), and the neural progenitor marker *NESTIN* was expressed similarly under all conditions (Figure S1D). These results indicate that neural induction is unaffected by Wnt, RA, or Shh signaling.

Modulation of the A-P Identity of PSC-Derived Neural Progenitors by Wnt and RA Signaling

We next examined the expression of A-P markers (Figure 2A) in ESC-derived neurospheres by qRT-PCR (Figure 2B). IWP-2-treated neurospheres expressed high levels of the forebrain markers *FOXG1* and *SIX3* (Oliver et al., 1995; Xuan et al., 1995). The expression levels of the forebrain/midbrain markers *OTX1* and *OTX2* (Simeone et al., 1992) were highest in untreated neurospheres. The low expression level of *OTX1* in IWP-2-treated neurospheres agrees with the observation that this gene is not expressed in the anterior-most region of the forebrain (Shimamura et al., 1997). *EN1*, which is expressed in the midbrain and the anterior hindbrain (Hanks et al., 1995), was highly expressed in neurospheres treated with CHIR at concentrations of 0.5 and 1 μM. *HOXB4* and *HOXC4*, markers of the posterior hindbrain and the spinal cord (Hunt et al., 1991), were expressed primarily in cultures exposed to 3 μM CHIR, and their expression levels were enhanced further by the addition of RA. These results indicate that the posteriorization of neural progenitors is driven by activation of the Wnt and RA signaling pathways.

The regulation of marker expression correlating with the A-P axis was also confirmed by immunocytochemical analysis for the FOXG1, OTX1, and HOXB4 proteins (Figure 2C). Furthermore, we confirmed the robustness of our protocol by using the 201B7 and 253G1 iPSC lines (Nakagawa et al., 2008; Takahashi et al., 2007). In both of these iPSC lines, the expression levels of the A-P markers in the neurospheres were similar to those in ESC-derived neurospheres (Figure S2). These results suggest that the

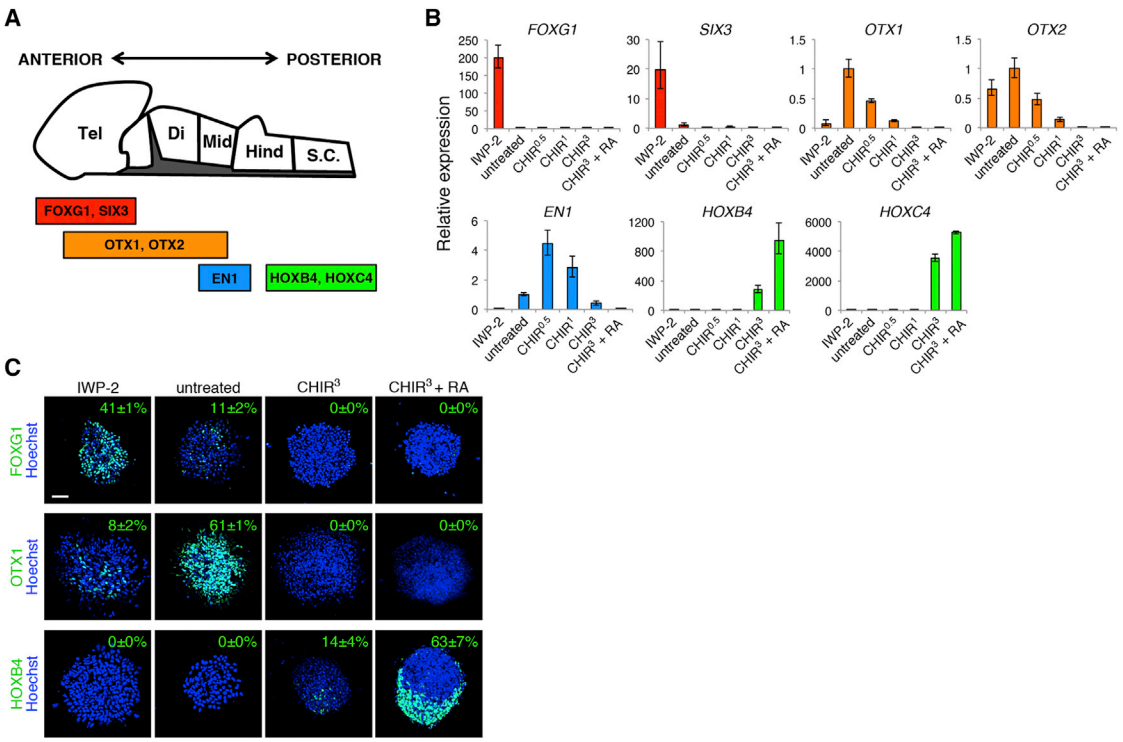

Figure 2. A-P Patterning by Modifying Wnt and RA Signaling

(A) Expression of A-P markers in the neural tube in vivo.

(B) qRT-PCR analysis of neurospheres for A-P marker expression (n = 3 independent experiments, mean ± SEM). Activation of Wnt and RA signaling posteriorized the neurospheres, whereas blockade of Wnt signaling anteriorized the neurospheres.

(C) Immunocytochemical analysis of neurospheres for A-P markers. The frequency of neurospheres containing immunopositive cells is shown as the percentage of total neurospheres (n = 3 independent experiments, mean ± SEM). A-P patterning was also confirmed at the protein level. Scale bar, 50 μm).

See also Table S1.

A-P identity of PSC-derived neural progenitors can be controlled by IWP-2, CHIR, and RA during neurosphere formation.

Control of the D-V Identity of PSC-Derived Neural Progenitors by Shh Signaling

In addition to the A-P identity, we next attempted to control the D-V identity by modulating Shh signaling. We hypothesized that neural progenitors derived from PSCs are dorsalized in the absence of Shh and that the activation of Shh signaling ventralizes neural progenitors with no influence on the A-P identity. To address this hypothesis, we assessed the expression levels of D-V makers in neurospheres by qRT-PCR analysis with the addition of Shh protein and purmorphamine (termed the "+Shh" group) (Figures 3A and 3B). We used these two Shh activators simultaneously because a previous report has demonstrated that co-treatment with Shh protein and purmorphamine was greatly superior to high concentrations of either of the two alone (Maroof et al., 2013). Other neurospheres received no exogenous ventralizing factors (termed the "−Shh" group).

The D-V markers *PAX6*, *PAX7*, *NKX2.1*, and *NKX2.2* are differentially expressed in vivo according to A-P and D-V positions (Figure 3A). *PAX6* is expressed dorsally in the forebrain, and the expression pattern also covers both the dorsal and the ventral portions of the posterior hindbrain and the spinal cord (Ericson et al., 1997; Osumi et al., 1997; Takahashi and Osumi, 2002; Walther and Gruss, 1991). In contrast, the midbrain and the anterior hindbrain lack *PAX6* expression (with the exception of the rhombic lip) (Engelkamp et al., 1999; Schwarz et al., 1999; Swanson et al., 2005; Yamasaki et al., 2001). *PAX7* is expressed throughout the dorsal part of the neural tube except for the anterior forebrain, where this gene is expressed only in the small dorsal-most region (Matsunaga et al., 2001). *NKX2.1* marks the ventral forebrain (Qiu et al., 1998), whereas *NKX2.2* is expressed ventrally throughout the A-P axis (Shimamura et al., 1995). Consistent with the in vivo expression patterns of these genes, *PAX6* was highly

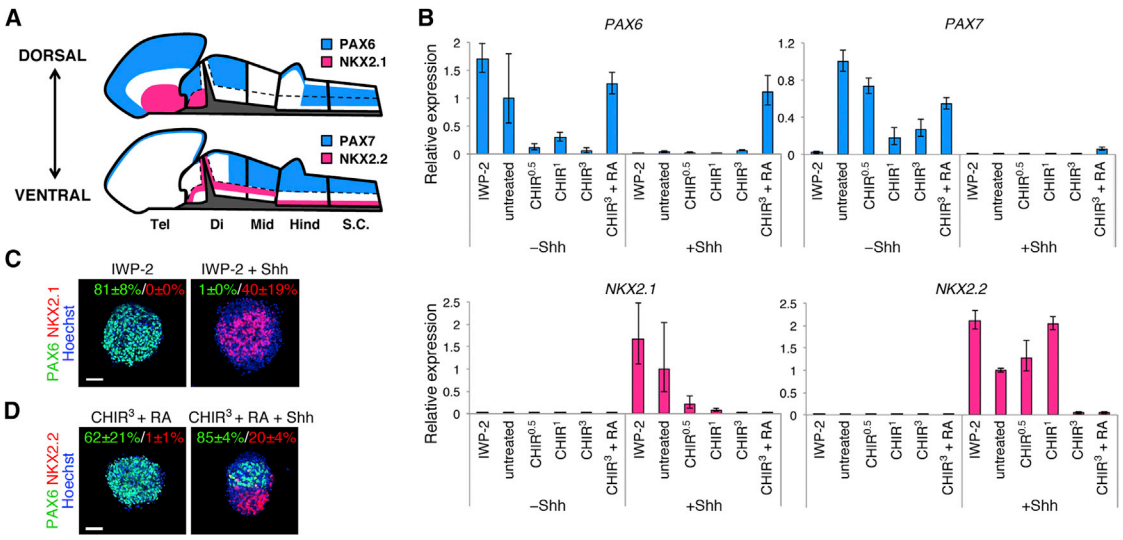

Figure 3. D-V Patterning by Treatment with Shh

(A) Expression of D-V markers in the neural tube. The dashed line indicates the alar-basal boundary.

(B) qRT-PCR analysis of neurospheres for D-V marker expression (n = 3 independent experiments, mean ± SEM). Neurospheres not treated with Shh showed a dorsal identity, whereas Shh treatment ventralized the neurospheres.

(C and D) Immunocytochemical analysis of neurospheres for PAX6/NKX2.1 (C) and PAX6/NKX2.2 (D). The frequency of neurospheres containing immunopositive cells is shown as the percentage of total neurospheres (n = 3 independent experiments, mean ± SEM). D-V patterning was also confirmed at the protein level. Scale bars, 50 μm.

See also Table S1.

expressed in neurospheres with forebrain characteristics (i.e., IWP-2-treated and untreated neurospheres) in the −Shh group as well as those with the characteristics of the posterior hindbrain and the spinal cord (i.e., $CHIR^3$+RA-treated neurospheres). Only the latter maintained *PAX6* expression after Shh activation. Meanwhile, *PAX7* was upregulated in the −Shh group, except under the IWP-2-treated condition, whereas *PAX7* expression was low under all conditions in the +Shh group. *NKX2.1* was expressed primarily in neurospheres with forebrain characteristics (IWP-2-treated and untreated) in the +Shh group. The expression of *NKX2.2* was generally high in the +Shh group. The relatively low expression level of *NKX2.2* in neurospheres with posterior characteristics in the +Shh group agrees with the fact that *NKX2.2* expression is initially only seen in the anterior part of the neural tube and then gradually extends to the spinal cord (Shimamura et al., 1995).

The control of the D-V axis shown by qRT-PCR analysis was also confirmed by immunocytochemical analysis for the PAX6, NKX2.1, and NKX2.2 proteins (Figures 3C and 3D). Moreover, D-V regulation was reproduced readily in the iPSC lines (Figure S2). Our results indicate that the D-V identity of PSC-derived neural progenitors can be controlled without perturbing the A-P identity.

Recapitulation of Telencephalic D-V Patterning

To further confirm the D-V control, we examined the expression of telencephalon-specific D-V markers (Figure 4A). *EMX1/2* and *DLX2* are confined to the dorsal and the ventral telencephalon, respectively (with the exception of small diencephalic regions) (Porteus et al., 1991; Simeone et al., 1992). Although the proneural genes *NGN2* and *ASCL1* are expressed in various regions of the neural tube, a D-V bias in their expression is clearly observed in the telencephalon (Fode et al., 2000). *EMX1/2* and *NGN2* were significantly upregulated in IWP-2-treated neurospheres without Shh activation. In contrast, the expression of *DLX2* and *ASCL1* was increased by Shh activation. These data provide additional evidence for the D-V control of PSC-derived neural progenitors.

Differentiation of Neural Progenitors into Specific Neuronal Subtypes in Accordance with Regional Identity

To investigate whether the regional identity of neural progenitors was retained upon differentiation into neurons, neurospheres were subjected to a neural differentiation protocol (Figure 1B). Our protocol predominantly produced neurons rather than astrocytes or oligodendrocytes (Figure S3A). We examined the expression of synapse markers and the intracellular calcium level during electrical

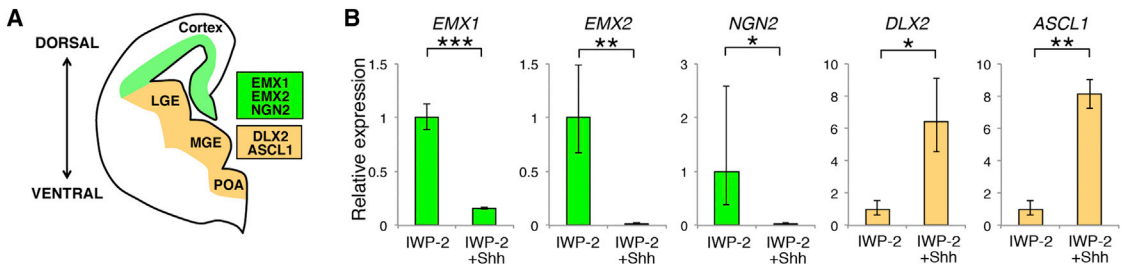

Figure 4. Telencephalic D-V Patterning

(A) Expression of D-V markers in the telencephalon. MGE, medial ganglionic eminence; LGE, lateral ganglionic eminence; POA, preoptic area.

(B) qRT-PCR analysis of neurospheres for telencephalic D-V marker expression (n = 3–4 independent experiments; mean ± SEM; *p < 0.05, **p < 0.01, ***p < 0.001; Student's t test).

field stimulation (Figures S3B–S3D). These results indicate that neurons derived by our protocol were functional regardless of the experimental conditions.

We determined the A-P identity of neurosphere-differentiated neurons (Figure 5A). Neurons generated from IWP-2-treated neurospheres expressed high levels of the forebrain cortical neuronal marker *TBR1* (Bulfone et al., 1995). *GATA3*, expressed from the diencephalon to the hindbrain (George et al., 1994), was upregulated at low CHIR concentrations (0–1 μM). *LBX1*, which marks dorsal neurons in the hindbrain and the spinal cord (Jagla et al., 1995), was highly expressed in neurons differentiated from CHIR^3+RA-treated neurospheres. These results imply that neural progenitors retain their A-P identity in differentiated neuronal cultures.

We next examined the D-V identity of differentiated neurons (Figures 5B–5F). In the telencephalon, TBR1+ cortical neurons are born dorsally, whereas the ventral area produces cortical interneurons, which is marked by *LHX6* and *LHX*8 expression (Marín and Rubenstein, 2001). As expected, the expression level of *TBR1* was elevated in neurons generated from IWP-2-treated neurospheres and decreased by activation of Shh signaling (Figures 5B and 5E). In contrast, *LHX6* and *LHX8* were significantly upregulated by Shh activation (Figure 5B). Dopaminergic and serotonergic neurons are selectively derived from the ventral portion of the midbrain and the hindbrain, respectively (Goridis and Rohrer, 2002). Although the gene expression of the dopamine-synthesizing enzyme *TH* did not change significantly, that of *LMX1A* and *FOXA2*, master transcriptional regulators of dopaminergic neuronal differentiation (Andersson et al., 2006; Ferri et al., 2007), was upregulated markedly by Shh activation under the 0.5 μM CHIR-treated condition (Figure 5C; Figure S4A). We also detected high expression of the serotonergic neuronal marker *PET1* (Hendricks et al., 1999) concomitantly with a small population of cells that were immunopositive for serotonin (Figure 5C; Figure S4C). Furthermore, *VMAT2* and *AADC*, markers for both dopaminergic and serotonergic neurons (Flames and Hobert, 2011), were upregulated (Figure S4A). *LHX9*, which marks d1 neurons in the dorsal spinal cord (Liem et al., 1997), was highly expressed in neurons generated from CHIR^3+RA-treated neurospheres, whereas the expression of *HB9*, which marks motor neurons in the ventral spinal cord (Arber et al., 1999), was elevated by ventralization via Shh activation (Figures 5D and 5F). *CHT*, an additional spinal cord motor neuron marker that is essential for the uptake of choline into motor neurons (Okuda et al., 2000), was also upregulated (Figure S4B).

Finally, we tested whether neural crest-derived peripheral neurons were induced. The peripheral neuron marker Peripherin (Escurat et al., 1990) was not detected under almost all conditions. However, approximately 20% of neurons were immunopositive for this marker under the CHIR^3+RA-treated and CHIR^3+RA+Shh-treated conditions. Under the CHIR^3+RA-treated condition, BRN3A, an additional peripheral neuron marker (Fedtsova and Turner, 1995), was also expressed in a portion of Peripherin+ neurons (Figure S4D). Given that neural crest cells originate from the dorsal-most region of the neural tube (Knecht and Bronner-Fraser, 2002), these results are consistent with their dorsal identity. Under the CHIR^3+RA+Shh-treated condition, however, Peripherin+ neurons expressed the motor neuron marker SMI-32 (Carriedo et al., 1996). This result is consistent with the fact that Peripherin is expressed not only in peripheral neurons but also in spinal cord motor neurons (Escurat et al., 1990). In summary, both the A-P and D-V identities acquired in the neural progenitor stage were maintained throughout neuronal differentiation in culture, and neural progenitors were able to differentiate into specific neuronal subtypes in accordance with their regional identities.

Reproduction of Subtype-Specific Disease Phenotypes In Vitro

In most neurological diseases, specific neuronal subtypes are selectively impaired. For example, spinal cord motor

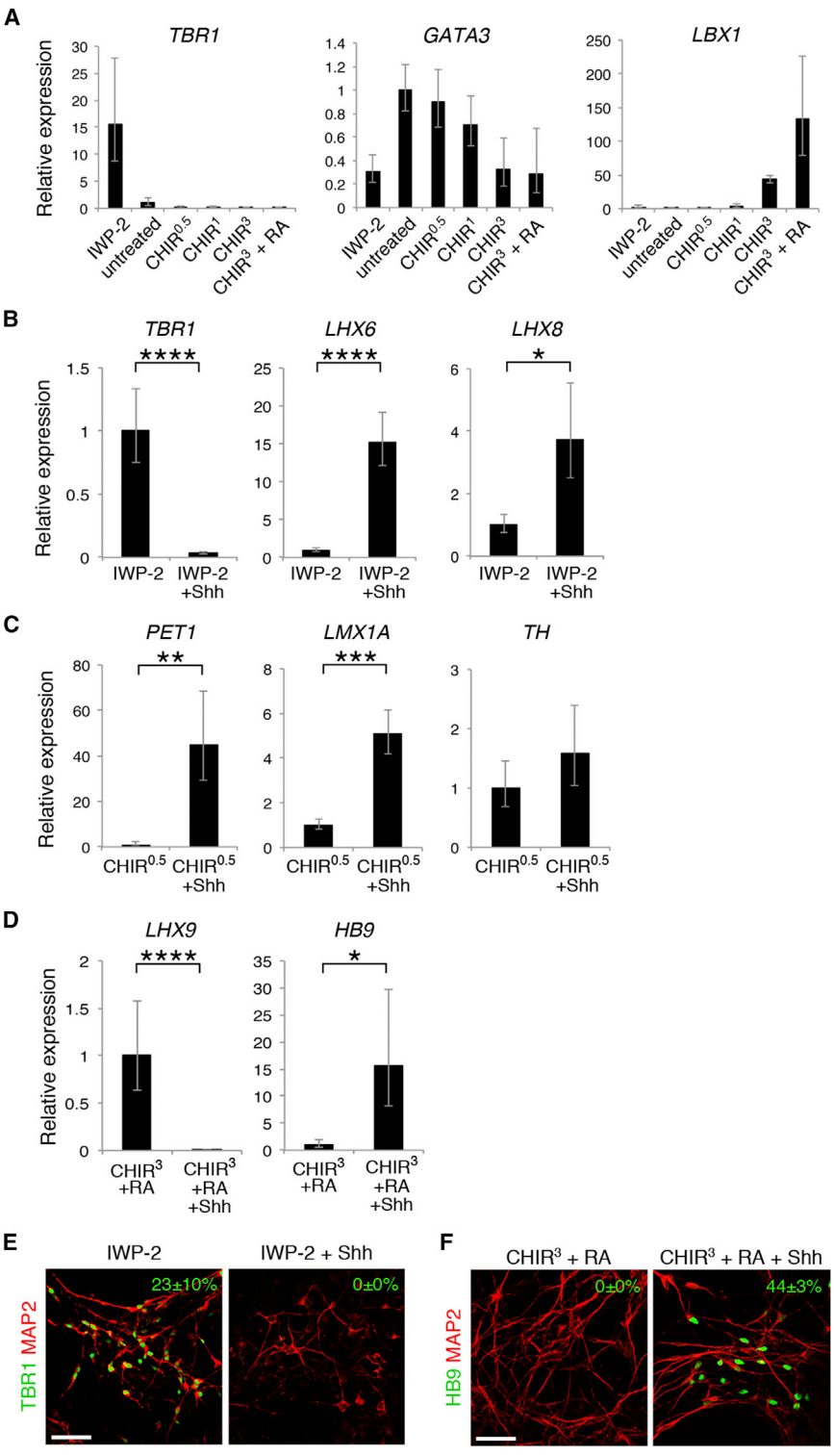

Figure 5. Generation of Region-Specific Neuronal Subtypes

(A) qRT-PCR analysis of neurosphere-derived neurons for *TBR1*, *GATA3*, and *LBX1* expression (n = 4–5 independent experiments, mean ± SEM). A-P patterning was maintained throughout neuronal differentiation in vitro.

(B–D) qRT-PCR analysis of neurosphere-derived neurons for the expression of neuronal subtype markers expressed in the forebrain (B), the mid/hindbrain (C), and the spinal cord (D) (n = 5–7 independent experiments; mean ± SEM; *p < 0.05, **p < 0.01, ***p < 0.001, ****p < 0.0001; Student's t test). Neurospheres differentiated into specific neuronal subtypes in accordance with their regional identity.

(E and F) Immunocytochemical analysis of neurosphere-derived neurons for TBR1 (E) and HB9 (F). The frequency of immunopositive cells is shown as the percentage of MAP2+ neurons (n = 3 independent experiments, mean ± SEM). Scale bars, 50 μm.

See also Table S1.

neurons are selectively damaged in ALS (Bruijn et al., 2004), and forebrain cortical neurons are preferentially affected in AD (Braak and Braak, 1991; Morrison and Hof, 1997; Thal et al., 2002). Although this subtype specificity probably plays an important role in pathology, its mechanism remains to be elucidated. Particularly in PSC-based disease models, most previous reports have focused only on the disease-susceptible neuronal subtype,

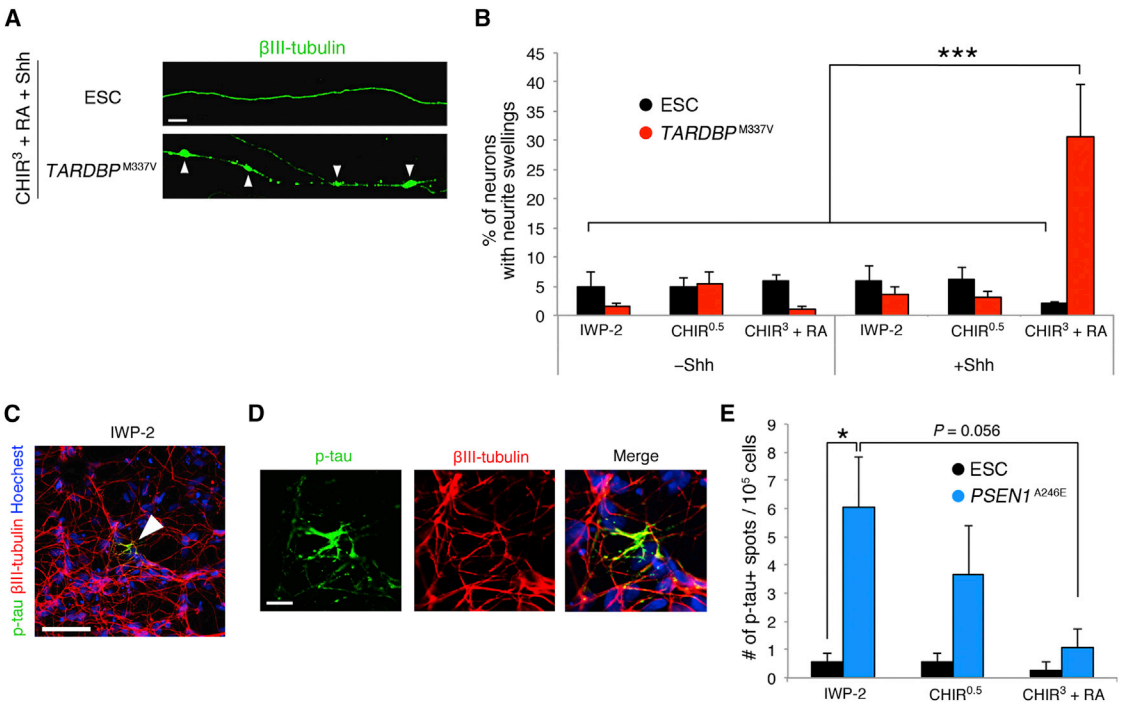

Figure 6. Reproduction of Subtype-Specific Disease Phenotypes In Vitro

(A) Representative images of neurites from PSC-derived neurons with the characteristics of the ventral spinal cord ($CHIR^3$+RA+Shh-treated). ALS iPSC-derived neurons exhibited swollen neurites (arrowheads). Scale bar, 10 μm.

(B) Quantification of neurons with neurite swellings (n = 3 independent experiments, mean ± SEM, ***p < 0.001, ANOVA with Tukey's test). ALS iPSC-derived neurons with the characteristics of the ventral spinal cord were remarkably damaged.

(C) Immunocytochemical analysis of AD iPSC-derived neurons with forebrain characteristics (IWP-2-treated). Accumulation of p-tau was observed in the AD iPSC cultures (arrowhead). Scale bar, 50 μm.

(D) Higher-magnification images of the immunoreactive p-tau+ spots shown in (C). Scale bar, 10 μm.

(E) Quantification of p-tau+ spots (n = 3 independent experiments, mean ± SEM, *p < 0.05, ANOVA with Tukey's test). Accumulation of p-tau was increased in AD iPSC-derived neurons with forebrain characteristics.

and other aspects of subtype specificity have yet to be explored.

Our first aim was to test whether disease subtype specificity can be recapitulated in vitro by using PSCs. We derived neurons from disease-specific iPSC lines via our protocol described above. Here we used ALS and AD iPSC lines carrying *TARDBP*^{M337V} and *PSEN1*^{A246E}/*PSEN2*^{N141I} mutations, respectively (Egawa et al., 2012; Yagi et al., 2011), and the control of regional identity was confirmed in neurospheres derived from each iPSC line (Figure S5).

In the ALS iPSC-derived neurons, neurite swellings were observed preferentially in neurons with the characteristics of the ventral spinal cord generated from $CHIR^3$+RA+Shh-treated neurospheres (Figures 6A and 6B). In contrast, neurons with other regional identities rarely exhibited swellings. Because neurite swellings (or "spheroids") are a feature of neuronal cell dysfunction in ALS (Delisle and Carpenter, 1984), these observations suggest that ventral spinal cord-specific phenotypes of ALS were recapitulated successfully in our system. Next, we tried to demonstrate motor neuron specificity among the ventral spinal cord subtypes by labeling motor neurons with the fluorescence protein (Venus) reporter under control of the *HB9* promoter. However, the cells showed fluorescence labeling of only the soma and proximal neurites, probably because of weak intracellular diffusion of the Venus protein. Consequently, we failed to identify neurite swellings distal to the soma in *HB9*-Venus-positive neurons (data not shown). Therefore, currently, we cannot eliminate the possibility that subtypes other than motor neurons in the ventral spinal cord were also affected by neurite swellings. Indeed, several recent reports indicate that spinal cord interneurons are implicated in ALS pathology (reviewed in Turner and Kiernan, 2012).

In AD iPSC-derived neurons, we found spot-like accumulations of p-tau (Figures 6C and 6D). The number of p-tau+ spots increased in neurons with forebrain characteristics generated from IWP-2-treated neurospheres compared

with the $CHIR^3$+RA condition corresponding to the spinal cord (Figure 6E; Figure S6A). To eliminate the possibility that the addition of CHIR during the neurosphere stage led to inhibition of GSK3β-mediated tau phosphorylation in the differentiation stage, we next measured GSK3β activity in differentiated neurons by quantifying nuclear β-catenin intensity. We confirmed that β-catenin intensity remained relatively constant under all conditions and that residual CHIR had no effect on tau phosphorylation in the differentiation stage (Figure S6B). These results indicate that a characteristic feature of AD pathology, i.e., p-tau accumulation, was reproduced in a region-specific manner. Taken together, our findings show that the subtype specificity of neurological disease phenotypes can be modeled in vitro by defining the regional identity of PSC-derived neural progenitors and neurons.

DISCUSSION

In this study, we established a culture system for controlling the regional identity of PSC-derived neural progenitors and neurons based on an identical protocol. Simple treatment with three factors, IWP-2, CHIR, and RA, effectively patterned the A-P identity, ranging from the telencephalon to the spinal cord. In addition, Shh activation converted the D-V identity from dorsal into ventral without perturbing the A-P identity. Furthermore, subtype-specific ALS and AD phenotypes were reproduced in vitro by using the described protocol.

Our findings are consistent with previous reports demonstrating that the graded signaling activities of Wnt/RA and Shh establish the A-P and D-V axes in vivo. Also noteworthy is that our study shows that this model for early neural patterning, which is proposed mostly from work on *Xenopus*, chicks, and mice, can be applied to human development. Because in vivo experiments of the human embryo are ethically challenging and technically difficult, our culture system now provides novel opportunities to uncover the mechanism of neural patterning in humans.

A remaining issue regarding our present culture system is the ability to recapitulate the environment after regional specification. In some neuronal subtypes, additional signals are needed for further specification, maturation, and maintenance. When cells migrate from their birthplace or if they project to distant targets, they often receive such signals from cells with different regional identity. Such additional signals cannot be recapitulated in our present culture system. In the case of midbrain dopaminergic neurons, for example, transforming growth factor β (TGF-β) expressed in their projection targets is necessary for their maintenance (Poulsen et al., 1994). Dopaminergic neurons in our culture did not express late-stage markers such as *PITX3* and *DAT*, probably because of the lack of such additional signals (data not shown). In addition to treatment with signaling modulators, co-culturing with cells of the destination of migration or cells of the projection targets would be a promising approach to overcome this issue.

Specific brain regions are preferentially damaged in most neurological diseases, whereas regions other than the lesioned area remain relatively unaffected. For this reason, the differentiation of patient-derived iPSCs into specific neuronal subtypes representing the lesion site is a valuable approach for modeling human neurological diseases (Imaizumi and Okano, 2014; Okano and Yamanaka, 2014). The current investigation reproduced p-tau accumulation as an AD phenotype by endowing neurons with forebrain characteristics. On the other hand, a previous report using the same iPSC clones did not detect such a phenotype, probably because of the induction of inappropriate subtypes (Yagi et al., 2011). These results highlight the importance of correct neuronal subtype specification in reproducing neurological disease phenotypes with PSCs.

Some investigators have reported the directed differentiation of PSCs into a limited number of neuronal subtypes, including midbrain dopaminergic neurons and spinal cord motor neurons (Kriks et al., 2011; Li et al., 2005). Given that each differentiation protocol is overly optimized for a particular subtype, the protocol in question cannot be readily applied to additional neuronal subtypes. Nevertheless, our culture system theoretically enables the differentiation of PSCs into all neuronal subtypes, making it possible to efficiently generate subtypes whose induction from PSCs has been difficult.

Also, as emphasized above, our culture system is based on the same protocol to obtain neuronal subtypes with equivalent efficiency and under the same general culture conditions (with the exception of the modulation of different signaling cascades). Therefore, our method allows comparative analysis of a variety of neuronal subtypes, whereas earlier investigations on disease modeling have focused only on selectively affected subtypes. Moreover, other investigators have reported that the modulation of Wnt signaling can direct the regional identity of PSC-derived neurons in a manner similar to that observed in our culture system. Nevertheless, a parallel analysis of disease phenotypes between neurons with different regional identities was not performed in these studies (Kirkeby et al., 2012; Moya et al., 2014). To fully understand the mechanism of disease pathology and progression, one must investigate not only the manner in which specific neuronal subtypes are affected but also how other subtypes remain unaffected. In the case of genetic diseases, neural subtype specificity of disease phenotypes is not necessarily accounted for by the

expression pattern of the responsible genes. For example, some mutations in *TARDBP*, which is globally expressed across the entire brain, cause motor neuron-selective degeneration (Kabashi et al., 2008, 2010; Sephton et al., 2010). Similarly, although *PSEN1* and *PSEN2* show widespread expression in the brain, their mutations predominantly affect forebrain neurons (Rogaev et al., 1995; Sherrington et al., 1995). However, the mechanism of neuronal subtype specificity of these disease phenotypes is unclear. Our culture system may permit investigations toward filling in the gaps in this knowledge base.

We do not yet know the mechanism of neuronal subtype specificity of various neurological disease phenotypes. Identification of factors enforcing pathogenesis in disease-susceptible subtypes or evading pathogenesis in insusceptible subtypes will help to clarify this. Regardless, our culture system will undoubtedly allow new insights into modeling neurological diseases with PSCs.

EXPERIMENTAL PROCEDURES

Culture of Undifferentiated ESCs and iPSCs

The human ESC (hESC) line KhES-1 (Suemori et al., 2006), the control human iPSC (hiPSC) lines 201B7 and 253G1 (Nakagawa et al., 2008; Takahashi et al., 2007), the ALS iPSC line A3411 (Egawa et al., 2012), and the AD iPSC lines PS1-2 and PS2-1 (Yagi et al., 2011) were cultured on mitomycin C-treated SNL murine fibroblast feeder cells in standard hESC medium (DMEM/F12, Sigma) containing 20% KnockOut serum (KSR) replacement (Life Technologies), 0.1 mM non-essential amino acids (Sigma), 0.1 mM 2-mercaptoethanol (Sigma), and 4 ng/ml fibroblast growth factor 2 (FGF-2) (PeproTech)) in an atmosphere containing 3% CO_2.

hESCs were used in accordance with the guidelines regarding the utilization of hESCs with approval from the Ministry of Education, Culture, Sports, Science, and Technology (MEXT) of Japan and the Keio University School of Medicine Ethics Committee. All experimental procedures for iPSCs derived from patients were approved by the Keio University School of Medicine Ethics Committee (approval no. 20080016).

Neuronal Induction

Neuronal induction of hESCs/iPSCs was performed as described previously (Chaddah et al., 2012), with slight modifications. Briefly, hESCs/iPSCs were pretreated for 6 days with 3 μM SB431542 (Tocris), 150 nM LDN193189 (StemRD), and 3 μM CHIR99021 (Stemgent). They were then dissociated and seeded at a density of 10 cells/μl in medium hormone mix (MHM) (Okada et al., 2004, 2008; Shimazaki et al., 2001) with selected growth factors and inhibitors under conditions of 4% O_2/5% CO_2. The growth factors and inhibitors included 10 ng/ml human leukemia inhibitory factor (LIF) (Nacalai Tesque), 20 ng/ml FGF-2, 1× B27 supplement (Invitrogen), 2 μM SB431542, and 10 μM Y-27632 (Calbiochem).

Defining the day on which neurosphere culture was started as day 0, the following additives were included in the neurosphere culture: 2 μM IWP-2 (Sigma), 0.5–3 μM CHIR99021, and 1 μM RA (Sigma) from days 0–12 and 100 ng/ml Shh-C24II (R&D Systems) and 1 μM purmorphamine (Calbiochem) from days 2–12. On day 12, neurospheres were replated en bloc on dishes coated with poly-ornithine and laminin and cultured under conditions of 5% CO_2. The medium was changed to MHM supplemented with 1× B27 and 1 μM DAPT (Sigma). DAPT was excluded in the AD phenotype experiments.

qRT-PCR

Total RNA was isolated with the RNeasy mini kit (QIAGEN) with DNase I treatment, and cDNA was prepared by using a ReverTraAce qPCR RT kit (Toyobo). The qRT-PCR analysis was performed with SYBR premix Ex TaqII (Takara Bio) on a ViiA 7 real-time PCR system (Applied Biosystems). Values were normalized to *ACTB*. Reactions were carried out in duplicate, and data were analyzed by using the comparative (ΔΔCt) method. Relative expression levels are presented as geometric means ± geometric SEM. The primer sets used in these experiments are listed in Table S2.

Immunocytochemistry

Cells were fixed with 4% paraformaldehyde for 15 min at room temperature and then washed three times with PBS. After incubating with blocking buffer (PBS containing 5% normal fetal bovine serum and 0.3% Triton X-100) for 1 hr at room temperature, the cells were incubated overnight at 4°C with primary antibodies diluted with blocking buffer. We used blocking buffer without Triton X-100 for O4 staining and buffer with 0.03% Triton X-100 for Synaptotagmin and VAMP2 staining. Details of the primary antibodies and the dilution conditions are listed in Table S3. The cells were again washed three times with PBS and incubated with secondary antibodies conjugated with Alexa Fluor 488, Alexa Fluor 555, or Alexa Fluor 647 (Life Technologies) and Hoechst33342 (Dojindo Laboratories) for 1 hr at room temperature. After washing three times with PBS and once with distilled water, samples were mounted on slides and examined by using a LSM-710 confocal laser-scanning microscope (Carl Zeiss). For anti-NKX2.2 antibody staining, biotinylated secondary antibodies (Jackson ImmunoResearch Laboratories) were used after exposure to 1% H_2O_2 for 30 min at room temperature to inactivate endogenous peroxidase. The signals were then enhanced by using the Vectastain ABC kit (Vector Laboratories), followed by the TSA fluorescence system (PerkinElmer).

SUPPLEMENTAL INFORMATION

Supplemental Information includes Supplemental Experimental Procedures, six figures, and three tables and can be found with this article online at http://dx.doi.org/10.1016/j.stemcr.2015.10.005.

AUTHOR CONTRIBUTIONS

K. Imaizumi, W.A., and H.O. conceived and designed the project. K. Imaizumi and T.S. performed the experiments. K. Ibata and M.Y. performed the calcium imaging assays. K. Imaizumi and K.F. established the nuclear β-catenin intensity assay. K. Imaizumi, W.A., and H.O. interpreted the data and wrote the manuscript.

ACKNOWLEDGMENTS

We are grateful to Y. Okada (Aichi Medical University) and T. Matsumoto (Ajinomoto) for technical assistance, helpful advice, and discussions; T. Abe (Keio University) for statistical analysis; and all members of the H.O. laboratory for encouragement and kind support. We also thank Y. Okada for the HB9-Venus reporter, M. Itakura (Kitasato University) for antibodies, N. Nakatsuji and H. Suemori (Kyoto University) for hESC clones, S. Yamanaka and M. Nakagawa (Kyoto University) for hiPSC clones (253G1 and 201B7), H. Inoue (Kyoto University) for ALS iPSC clones, and N. Suzuki and D. Ito (Keio University) for AD iPSC clones. This work was supported by funding from the Project for the Realization of Regenerative Medicine and Support for Core Institutes for iPS Cell Research from the Ministry of Education, Culture, Sports, Science, and Technology of Japan (MEXT) (to H.O. and W.A.); the Research Center Network for Realization Research Centers/Projects of Regenerative Medicine (the Program for Intractable Disease Research utilizing disease-specific iPS Cells) from the Japan Science and Technology Agency (JST) and the Japan Agency for Medical Research and Development (AMED) (to H.O.); Scientific Research on Innovative Area, a MEXT Grant-in-Aid Project FY2014-2018 "Brain Protein Aging and Dementia Control" (to H.O.); New Energy and Industrial Technology Development Organization (to H.O. and W.A.); and the Keio University Medical Science Fund (to K. Imaizumi). H.O. is a paid scientific advisory board member for SanBio Co., Ltd.

Received: June 3, 2015
Revised: October 8, 2015
Accepted: October 8, 2015
Published: November 5, 2015

REFERENCES

Andersson, E., Tryggvason, U., Deng, Q., Friling, S., Alekseenko, Z., Robert, B., Perlmann, T., and Ericson, J. (2006). Identification of intrinsic determinants of midbrain dopamine neurons. Cell *124*, 393–405.

Andoh-Noda, T., Akamatsu, W., Miyake, K., Matsumoto, T., Yamaguchi, R., Sanosaka, T., Okada, Y., Kobayashi, T., Ohyama, M., Nakashima, K., et al. (2015). Differentiation of multipotent neural stem cells derived from Rett syndrome patients is biased toward the astrocytic lineage. Mol. Brain *8*, 31.

Arber, S., Han, B., Mendelsohn, M., Smith, M., Jessell, T.M., and Sockanathan, S. (1999). Requirement for the homeobox gene Hb9 in the consolidation of motor neuron identity. Neuron *23*, 659–674.

Braak, H., and Braak, E. (1991). Neuropathological stageing of Alzheimer-related changes. Acta Neuropathol. *82*, 239–259.

Brennand, K.J., Simone, A., Jou, J., Gelboin-Burkhart, C., Tran, N., Sangar, S., Li, Y., Mu, Y., Chen, G., Yu, D., et al. (2011). Modelling schizophrenia using human induced pluripotent stem cells. Nature *473*, 221–225.

Briscoe, J., and Ericson, J. (2001). Specification of neuronal fates in the ventral neural tube. Curr. Opin. Neurobiol. *11*, 43–49.

Bruijn, L.I., Miller, T.M., and Cleveland, D.W. (2004). Unraveling the mechanisms involved in motor neuron degeneration in ALS. Annu. Rev. Neurosci. *27*, 723–749.

Bulfone, A., Smiga, S.M., Shimamura, K., Peterson, A., Puelles, L., and Rubenstein, J.L. (1995). T-brain-1: a homolog of Brachyury whose expression defines molecularly distinct domains within the cerebral cortex. Neuron *15*, 63–78.

Bundo, M., Toyoshima, M., Okada, Y., Akamatsu, W., Ueda, J., Nemoto-Miyauchi, T., Sunaga, F., Toritsuka, M., Ikawa, D., Kakita, A., et al. (2014). Increased l1 retrotransposition in the neuronal genome in schizophrenia. Neuron *81*, 306–313.

Carriedo, S.G., Yin, H.Z., and Weiss, J.H. (1996). Motor neurons are selectively vulnerable to AMPA/kainate receptor-mediated injury in vitro. J. Neurosci. *16*, 4069–4079.

Chaddah, R., Arntfield, M., Runciman, S., Clarke, L., and van der Kooy, D. (2012). Clonal neural stem cells from human embryonic stem cell colonies. J. Neurosci. *32*, 7771–7781.

Chen, B., Dodge, M.E., Tang, W., Lu, J., Ma, Z., Fan, C.-W., Wei, S., Hao, W., Kilgore, J., Williams, N.S., et al. (2009). Small molecule-mediated disruption of Wnt-dependent signaling in tissue regeneration and cancer. Nat. Chem. Biol. *5*, 100–107.

Delisle, M.B., and Carpenter, S. (1984). Neurofibrillary axonal swellings and amyotrophic lateral sclerosis. J. Neurol. Sci. *63*, 241–250.

Devine, M.J., Ryten, M., Vodicka, P., Thomson, A.J., Burdon, T., Houlden, H., Cavaleri, F., Nagano, M., Drummond, N.J., Taanman, J.-W., et al. (2011). Parkinson's disease induced pluripotent stem cells with triplication of the α-synuclein locus. Nat. Commun. *2*, 440.

Dimos, J.T., Rodolfa, K.T., Niakan, K.K., Weisenthal, L.M., Mitsumoto, H., Chung, W., Croft, G.F., Saphier, G., Leibel, R., Goland, R., et al. (2008). Induced pluripotent stem cells generated from patients with ALS can be differentiated into motor neurons. Science *321*, 1218–1221.

Egawa, N., Kitaoka, S., Tsukita, K., Naitoh, M., Takahashi, K., Yamamoto, T., Adachi, F., Kondo, T., Okita, K., Asaka, I., et al. (2012). Drug screening for ALS using patient-specific induced pluripotent stem cells. Sci. Transl. Med. *4*, 145ra104.

Engelkamp, D., Rashbass, P., Seawright, A., and van Heyningen, V. (1999). Role of Pax6 in development of the cerebellar system. Development *126*, 3585–3596.

Ericson, J., Rashbass, P., Schedl, A., Brenner-Morton, S., Kawakami, A., van Heyningen, V., Jessell, T.M., and Briscoe, J. (1997). Pax6 controls progenitor cell identity and neuronal fate in response to graded Shh signaling. Cell *90*, 169–180.

Escurat, M., Djabali, K., Gumpel, M., Gros, F., and Portier, M.M. (1990). Differential expression of two neuronal intermediate-filament proteins, peripherin and the low-molecular-mass neurofilament protein (NF-L), during the development of the rat. J. Neurosci. *10*, 764–784.

Fedtsova, N.G., and Turner, E.E. (1995). Brn-3.0 expression identifies early post-mitotic CNS neurons and sensory neural precursors. Mech. Dev. *53*, 291–304.

Ferri, A.L.M., Lin, W., Mavromatakis, Y.E., Wang, J.C., Sasaki, H., Whitsett, J.A., and Ang, S.L. (2007). Foxa1 and Foxa2 regulate multiple phases of midbrain dopaminergic neuron development in a dosage-dependent manner. Development *134*, 2761–2769.

Flames, N., and Hobert, O. (2011). Transcriptional control of the terminal fate of monoaminergic neurons. Annu. Rev. Neurosci. *34*, 153–184.

Fode, C., Ma, Q., Casarosa, S., Ang, S.L., Anderson, D.J., and Guillemot, F. (2000). A role for neural determination genes in specifying the dorsoventral identity of telencephalic neurons. Genes Dev. *14*, 67–80.

George, K.M., Leonard, M.W., Roth, M.E., Lieuw, K.H., Kioussis, D., Grosveld, F., and Engel, J.D. (1994). Embryonic expression and cloning of the murine GATA-3 gene. Development *120*, 2673–2686.

Goridis, C., and Rohrer, H. (2002). Specification of catecholaminergic and serotonergic neurons. Nat. Rev. Neurosci. *3*, 531–541.

Hanks, M., Wurst, W., Anson-Cartwright, L., Auerbach, A.B., and Joyner, A.L. (1995). Rescue of the En-1 mutant phenotype by replacement of En-1 with En-2. Science *269*, 679–682.

Hendricks, T., Francis, N., Fyodorov, D., and Deneris, E.S. (1999). The ETS domain factor Pet-1 is an early and precise marker of central serotonin neurons and interacts with a conserved element in serotonergic genes. J. Neurosci. *19*, 10348–10356.

Higurashi, N., Uchida, T., Lossin, C., Misumi, Y., Okada, Y., Akamatsu, W., Imaizumi, Y., Zhang, B., Nabeshima, K., Mori, M.X., et al. (2013). A human Dravet syndrome model from patient induced pluripotent stem cells. Mol. Brain *6*, 19.

Hook, V., Brennand, K.J., Kim, Y., Toneff, T., Funkelstein, L., Lee, K.C., Ziegler, M., and Gage, F.H. (2014). Human iPSC neurons display activity-dependent neurotransmitter secretion: aberrant catecholamine levels in schizophrenia neurons. Stem Cell Reports *3*, 531–538.

Hunt, P., Gulisano, M., Cook, M., Sham, M.H., Faiella, A., Wilkinson, D., Boncinelli, E., and Krumlauf, R. (1991). A distinct Hox code for the branchial region of the vertebrate head. Nature *353*, 861–864.

Imaizumi, Y., and Okano, H. (2014). Modeling human neurological disorders with induced pluripotent stem cells. J. Neurochem. *129*, 388–399.

Imaizumi, Y., Okada, Y., Akamatsu, W., Koike, M., Kuzumaki, N., Hayakawa, H., Nihira, T., Kobayashi, T., Ohyama, M., Sato, S., et al. (2012). Mitochondrial dysfunction associated with increased oxidative stress and α-synuclein accumulation in PARK2 iPSC-derived neurons and postmortem brain tissue. Mol. Brain *5*, 35.

Israel, M.A., Yuan, S.H., Bardy, C., Reyna, S.M., Mu, Y., Herrera, C., Hefferan, M.P., Van Gorp, S., Nazor, K.L., Boscolo, F.S., et al. (2012). Probing sporadic and familial Alzheimer's disease using induced pluripotent stem cells. Nature *482*, 216–220.

Jagla, K., Dollé, P., Mattei, M.G., Jagla, T., Schuhbaur, B., Dretzen, G., Bellard, F., and Bellard, M. (1995). Mouse Lbx1 and human LBX1 define a novel mammalian homeobox gene family related to the Drosophila lady bird genes. Mech. Dev. *53*, 345–356.

Jiao, J., Yang, Y., Shi, Y., Chen, J., Gao, R., Fan, Y., Yao, H., Liao, W., Sun, X.F., and Gao, S. (2013). Modeling Dravet syndrome using induced pluripotent stem cells (iPSCs) and directly converted neurons. Hum. Mol. Genet. *22*, 4241–4252.

Kabashi, E., Valdmanis, P.N., Dion, P., Spiegelman, D., McConkey, B.J., Vande Velde, C., Bouchard, J.-P., Lacomblez, L., Pochigaeva, K., Salachas, F., et al. (2008). TARDBP mutations in individuals with sporadic and familial amyotrophic lateral sclerosis. Nat. Genet. *40*, 572–574.

Kabashi, E., Lin, L., Tradewell, M.L., Dion, P.A., Bercier, V., Bourgouin, P., Rochefort, D., Bel Hadj, S., Durham, H.D., Vande Velde, C., et al. (2010). Gain and loss of function of ALS-related mutations of TARDBP (TDP-43) cause motor deficits in vivo. Hum. Mol. Genet. *19*, 671–683.

Kiecker, C., and Lumsden, A. (2012). The role of organizers in patterning the nervous system. Annu. Rev. Neurosci. *35*, 347–367.

Kirkeby, A., Grealish, S., Wolf, D.A., Nelander, J., Wood, J., Lundblad, M., Lindvall, O., and Parmar, M. (2012). Generation of regionally specified neural progenitors and functional neurons from human embryonic stem cells under defined conditions. Cell Rep. *1*, 703–714.

Knecht, A.K., and Bronner-Fraser, M. (2002). Induction of the neural crest: a multigene process. Nat. Rev. Genet. *3*, 453–461.

Kondo, T., Asai, M., Tsukita, K., Kutoku, Y., Ohsawa, Y., Sunada, Y., Imamura, K., Egawa, N., Yahata, N., Okita, K., et al. (2013). Modeling Alzheimer's disease with iPSCs reveals stress phenotypes associated with intracellular Aβ and differential drug responsiveness. Cell Stem Cell *12*, 487–496.

Kriks, S., Shim, J.-W., Piao, J., Ganat, Y.M., Wakeman, D.R., Xie, Z., Carrillo-Reid, L., Auyeung, G., Antonacci, C., Buch, A., et al. (2011). Dopamine neurons derived from human ES cells efficiently engraft in animal models of Parkinson's disease. Nature *480*, 547–551.

Li, X.J., Du, Z.W., Zarnowska, E.D., Pankratz, M., Hansen, L.O., Pearce, R.A., and Zhang, S.C. (2005). Specification of motoneurons from human embryonic stem cells. Nat. Biotechnol. *23*, 215–221.

Liem, K.F., Jr., Tremml, G., and Jessell, T.M. (1997). A role for the roof plate and its resident TGFbeta-related proteins in neuronal patterning in the dorsal spinal cord. Cell *91*, 127–138.

Liu, Y., Lopez-Santiago, L.F., Yuan, Y., Jones, J.M., Zhang, H., O'Malley, H.A., Patino, G.A., O'Brien, J.E., Rusconi, R., Gupta, A., et al. (2013). Dravet syndrome patient-derived neurons suggest a novel epilepsy mechanism. Ann. Neurol. *74*, 128–139.

Marchetto, M.C., and Gage, F.H. (2012). Modeling brain disease in a dish: really? Cell Stem Cell *10*, 642–645.

Marchetto, M.C.N., Carromeu, C., Acab, A., Yu, D., Yeo, G.W., Mu, Y., Chen, G., Gage, F.H., and Muotri, A.R. (2010). A model for neural development and treatment of Rett syndrome using human induced pluripotent stem cells. Cell *143*, 527–539.

Marín, O., and Rubenstein, J.L. (2001). A long, remarkable journey: tangential migration in the telencephalon. Nat. Rev. Neurosci. *2*, 780–790.

Maroof, A.M., Keros, S., Tyson, J.A., Ying, S.W., Ganat, Y.M., Merkle, F.T., Liu, B., Goulburn, A., Stanley, E.G., Elefanty, A.G., et al. (2013). Directed differentiation and functional maturation of cortical interneurons from human embryonic stem cells. Cell Stem Cell *12*, 559–572.

Marshall, H., Nonchev, S., Sham, M.H., Muchamore, I., Lumsden, A., and Krumlauf, R. (1992). Retinoic acid alters hindbrain Hox code and induces transformation of rhombomeres 2/3 into a 4/5 identity. Nature *360*, 737–741.

Matsunaga, E., Araki, I., and Nakamura, H. (2001). Role of Pax3/7 in the tectum regionalization. Development *128*, 4069–4077.

Mattis, V.B., and Svendsen, C.N. (2011). Induced pluripotent stem cells: a new revolution for clinical neurology? Lancet Neurol. *10*, 383–394.

Morrison, J.H., and Hof, P.R. (1997). Life and death of neurons in the aging brain. Science *278*, 412–419.

Moya, N., Cutts, J., Gaasterland, T., Willert, K., and Brafman, D.A. (2014). Endogenous WNT signaling regulates hPSC-derived neural progenitor cell heterogeneity and specifies their regional identity. Stem Cell Reports *3*, 1015–1028.

Nakagawa, M., Koyanagi, M., Tanabe, K., Takahashi, K., Ichisaka, T., Aoi, T., Okita, K., Mochiduki, Y., Takizawa, N., and Yamanaka, S. (2008). Generation of induced pluripotent stem cells without Myc from mouse and human fibroblasts. Nat. Biotechnol. *26*, 101–106.

Nguyen, H.N., Byers, B., Cord, B., Shcheglovitov, A., Byrne, J., Gujar, P., Kee, K., Schüle, B., Dolmetsch, R.E., Langston, W., et al. (2011). LRRK2 mutant iPSC-derived DA neurons demonstrate increased susceptibility to oxidative stress. Cell Stem Cell *8*, 267–280.

Nordström, U., Jessell, T.M., and Edlund, T. (2002). Progressive induction of caudal neural character by graded Wnt signaling. Nat. Neurosci. *5*, 525–532.

Okada, Y., Shimazaki, T., Sobue, G., and Okano, H. (2004). Retinoic-acid-concentration-dependent acquisition of neural cell identity during in vitro differentiation of mouse embryonic stem cells. Dev. Biol. *275*, 124–142.

Okada, Y., Matsumoto, A., Shimazaki, T., Enoki, R., Koizumi, A., Ishii, S., Itoyama, Y., Sobue, G., and Okano, H. (2008). Spatiotemporal recapitulation of central nervous system development by murine embryonic stem cell-derived neural stem/progenitor cells. Stem Cells *26*, 3086–3098.

Okano, H., and Yamanaka, S. (2014). iPS cell technologies: significance and applications to CNS regeneration and disease. Mol. Brain *7*, 22.

Okuda, T., Haga, T., Kanai, Y., Endou, H., Ishihara, T., and Katsura, I. (2000). Identification and characterization of the high-affinity choline transporter. Nat. Neurosci. *3*, 120–125.

Oliver, G., Mailhos, A., Wehr, R., Copeland, N.G., Jenkins, N.A., and Gruss, P. (1995). Six3, a murine homologue of the sine oculis gene, demarcates the most anterior border of the developing neural plate and is expressed during eye development. Development *121*, 4045–4055.

Osumi, N., Hirota, A., Ohuchi, H., Nakafuku, M., Iimura, T., Kuratani, S., Fujiwara, M., Noji, S., and Eto, K. (1997). Pax-6 is involved in the specification of hindbrain motor neuron subtype. Development *124*, 2961–2972.

Porteus, M.H., Bulfone, A., Ciaranello, R.D., and Rubenstein, J.L. (1991). Isolation and characterization of a novel cDNA clone encoding a homeodomain that is developmentally regulated in the ventral forebrain. Neuron *7*, 221–229.

Poulsen, K.T., Armanini, M.P., Klein, R.D., Hynes, M.A., Phillips, H.S., and Rosenthal, A. (1994). TGF beta 2 and TGF beta 3 are potent survival factors for midbrain dopaminergic neurons. Neuron *13*, 1245–1252.

Qiu, M., Shimamura, K., Sussel, L., Chen, S., and Rubenstein, J.L.R. (1998). Control of anteroposterior and dorsoventral domains of Nkx-6.1 gene expression relative to other Nkx genes during vertebrate CNS development. Mech. Dev. *72*, 77–88.

Ring, D.B., Johnson, K.W., Henriksen, E.J., Nuss, J.M., Goff, D., Kinnick, T.R., Ma, S.T., Reeder, J.W., Samuels, I., Slabiak, T., et al. (2003). Selective glycogen synthase kinase 3 inhibitors potentiate insulin activation of glucose transport and utilization in vitro and in vivo. Diabetes *52*, 588–595.

Rogaev, E.I., Sherrington, R., Rogaeva, E.A., Levesque, G., Ikeda, M., Liang, Y., Chi, H., Lin, C., Holman, K., Tsuda, T., et al. (1995). Familial Alzheimer's disease in kindreds with missense mutations in a gene on chromosome 1 related to the Alzheimer's disease type 3 gene. Nature *376*, 775–778.

Schwarz, M., Alvarez-Bolado, G., Dressler, G., Urbánek, P., Busslinger, M., and Gruss, P. (1999). Pax2/5 and Pax6 subdivide the early neural tube into three domains. Mech. Dev. *82*, 29–39.

Sephton, C.F., Good, S.K., Atkin, S., Dewey, C.M., Mayer, P., 3rd, Herz, J., and Yu, G. (2010). TDP-43 is a developmentally regulated protein essential for early embryonic development. J. Biol. Chem. *285*, 6826–6834.

Sherrington, R., Rogaev, E.I., Liang, Y., Rogaeva, E.A., Levesque, G., Ikeda, M., Chi, H., Lin, C., Li, G., Holman, K., et al. (1995). Cloning of a gene bearing missense mutations in early-onset familial Alzheimer's disease. Nature *375*, 754–760.

Shimamura, K., Hartigan, D.J., Martinez, S., Puelles, L., and Rubenstein, J.L. (1995). Longitudinal organization of the anterior neural plate and neural tube. Development *121*, 3923–3933.

Shimamura, K., Martinez, S., Puelles, L., and Rubenstein, J.L. (1997). Patterns of gene expression in the neural plate and neural tube subdivide the embryonic forebrain into transverse and longitudinal domains. Dev. Neurosci. *19*, 88–96.

Shimazaki, T., Shingo, T., and Weiss, S. (2001). The ciliary neurotrophic factor/leukemia inhibitory factor/gp130 receptor complex operates in the maintenance of mammalian forebrain neural stem cells. J. Neurosci. *21*, 7642–7653.

Simeone, A., Acampora, D., Gulisano, M., Stornaiuolo, A., and Boncinelli, E. (1992). Nested expression domains of four homeobox genes in developing rostral brain. Nature *358*, 687–690.

Sinha, S., and Chen, J.K. (2006). Purmorphamine activates the Hedgehog pathway by targeting Smoothened. Nat. Chem. Biol. *2*, 29–30.

Suemori, H., Yasuchika, K., Hasegawa, K., Fujioka, T., Tsuneyoshi, N., and Nakatsuji, N. (2006). Efficient establishment of human embryonic stem cell lines and long-term maintenance with stable karyotype by enzymatic bulk passage. Biochem. Biophys. Res. Commun. *345*, 926–932.

Swanson, D.J., Tong, Y., and Goldowitz, D. (2005). Disruption of cerebellar granule cell development in the Pax6 mutant, Sey mouse. Brain Res. Dev. Brain Res. *160*, 176–193.

Takahashi, M., and Osumi, N. (2002). Pax6 regulates specification of ventral neurone subtypes in the hindbrain by establishing progenitor domains. Development *129*, 1327–1338.

Takahashi, K., Tanabe, K., Ohnuki, M., Narita, M., Ichisaka, T., Tomoda, K., and Yamanaka, S. (2007). Induction of pluripotent stem cells from adult human fibroblasts by defined factors. Cell *131*, 861–872.

Thal, D.R., Rüb, U., Orantes, M., and Braak, H. (2002). Phases of A beta-deposition in the human brain and its relevance for the development of AD. Neurology *58*, 1791–1800.

Turner, M.R., and Kiernan, M.C. (2012). Does interneuronal dysfunction contribute to neurodegeneration in amyotrophic lateral sclerosis? Amyotroph. Lateral Scler. *13*, 245–250.

Walther, C., and Gruss, P. (1991). Pax-6, a murine paired box gene, is expressed in the developing CNS. Development *113*, 1435–1449.

Xuan, S., Baptista, C.A., Balas, G., Tao, W., Soares, V.C., and Lai, E. (1995). Winged helix transcription factor BF-1 is essential for the development of the cerebral hemispheres. Neuron *14*, 1141–1152.

Yagi, T., Ito, D., Okada, Y., Akamatsu, W., Nihei, Y., Yoshizaki, T., Yamanaka, S., Okano, H., and Suzuki, N. (2011). Modeling familial Alzheimer's disease with induced pluripotent stem cells. Hum. Mol. Genet. *20*, 4530–4539.

Yamasaki, T., Kawaji, K., Ono, K., Bito, H., Hirano, T., Osumi, N., and Kengaku, M. (2001). Pax6 regulates granule cell polarization during parallel fiber formation in the developing cerebellum. Development *128*, 3133–3144.

Stem Cell Reports, Volume *5*

Supplemental Information

Controlling the Regional Identity of hPSC-Derived Neurons to Uncover Neuronal Subtype Specificity of Neurological Disease Phenotypes

Kent Imaizumi, Takefumi Sone, Keiji Ibata, Koki Fujimori, Michisuke Yuzaki, Wado Akamatsu, and Hideyuki Okano

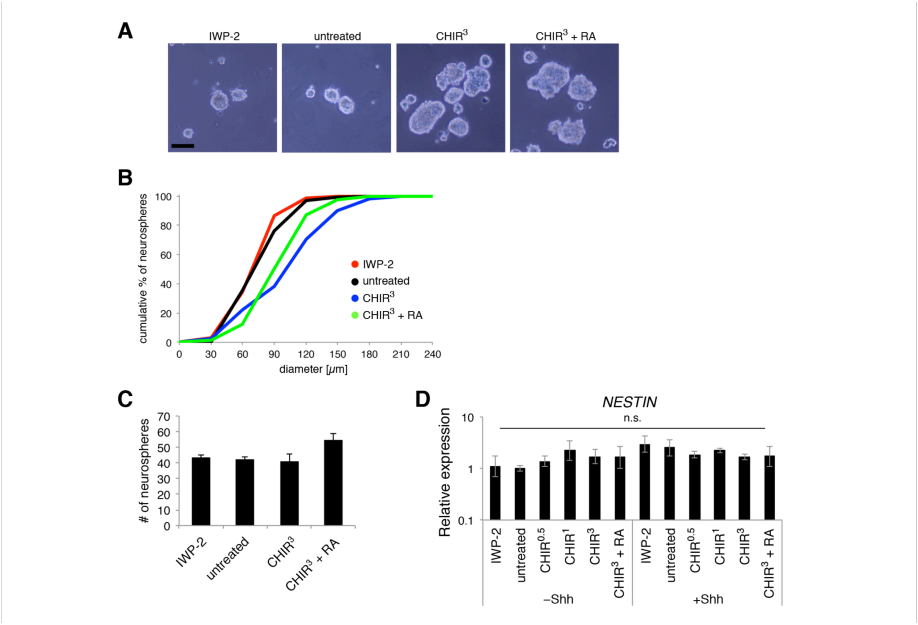

Figure S1. Patterning factors promoted expansion of neurospheres, but had no effect on neural induction

(A) Representative images of neurospheres (scale bar = 100 μm).

(B) Quantification of the size distribution of IWP-2, CHIR, and RA-treated neurospheres. While IWP-2 had no effect, the treatment of CHIR and RA promoted expansion of neurospheres.

(C) Quantification of the number of neurospheres (n = 3 technical replicates).

(D) qRT-PCR analysis of neurospheres for *NESTIN* expression (n = 3 independent experiments; mean ± SEM; n.s., not significant; ANOVA). Uniform expression of *NESTIN* confirmed that neural induction was unaffected by patterning factors.

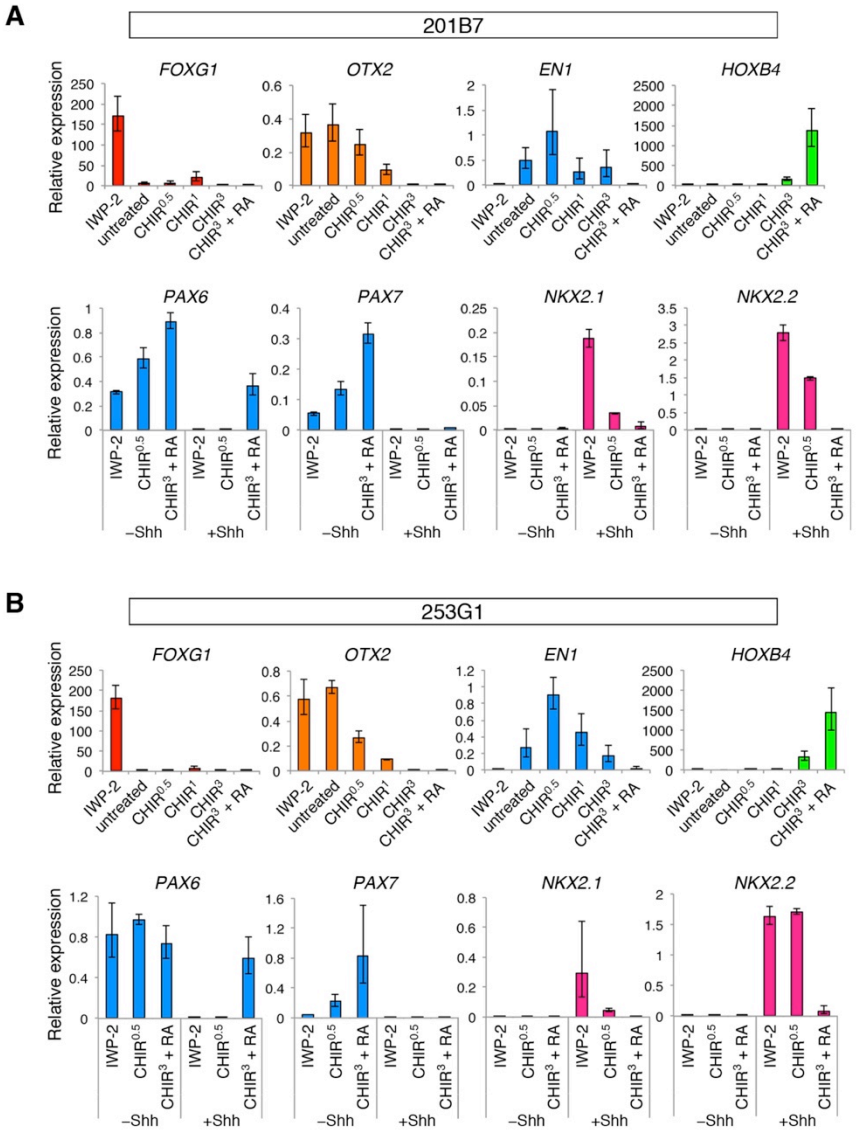

Figure S2. Region control was reproduced in iPSCs

(A) qRT-PCR analysis of 201B7-derived neurospheres for A-P and D-V markers expression relative to the untreated condition of KhES-1 (n = 3–4 independent experiments; mean ± SEM).

(B) qRT-PCR analysis of 253G1-derived neurospheres for A-P and D-V markers expression relative to the untreated condition of KhES-1 (n = 3 independent experiments; mean ± SEM).

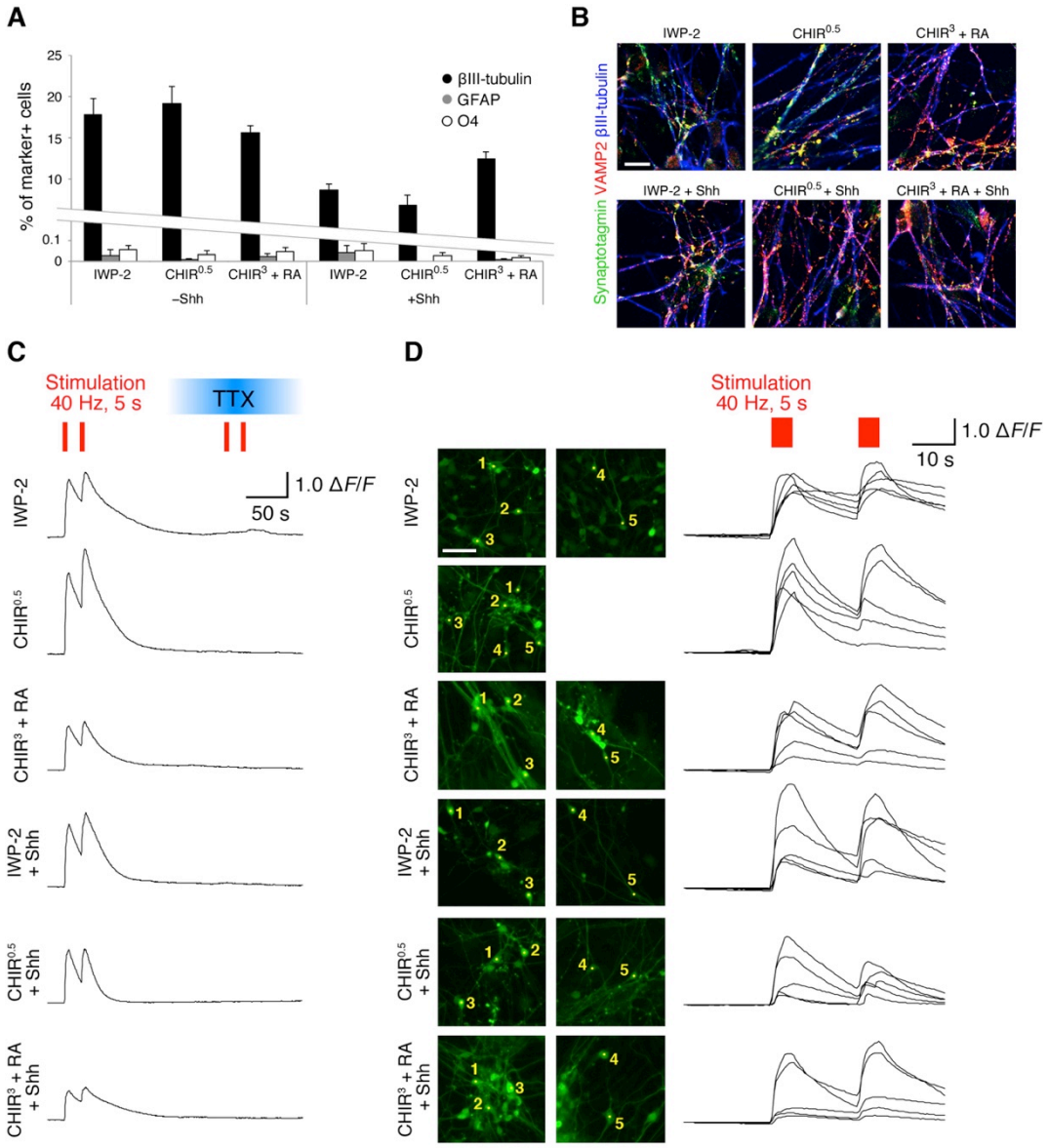

Figure S3. Differentiation capacity and neuronal functionality

(A) Quantification of the number of neurosphere-derived neurons, astrocytes, and oligodendrocytes (n = 3 independent experiments; mean ± SEM.). Neurospheres preferentially differentiated into neurons rather than astrocytes or oligodendrocytes.

(B) Immunocytochemical analysis of ESC-derived neurons for synapse markers (scale bar = 10 μm). The expression of synaptotagmin and VAMP2 was identified in each

condition.

(C) Traces of intracellular calcium signals. Calcium surges were induced by field stimulation and blocked by TTX.

(D) Traces of intracellular calcium signals in five cells. Cells 1–5 correspond to individual cells analyzed by calcium imaging (scale bar = 50 μm).

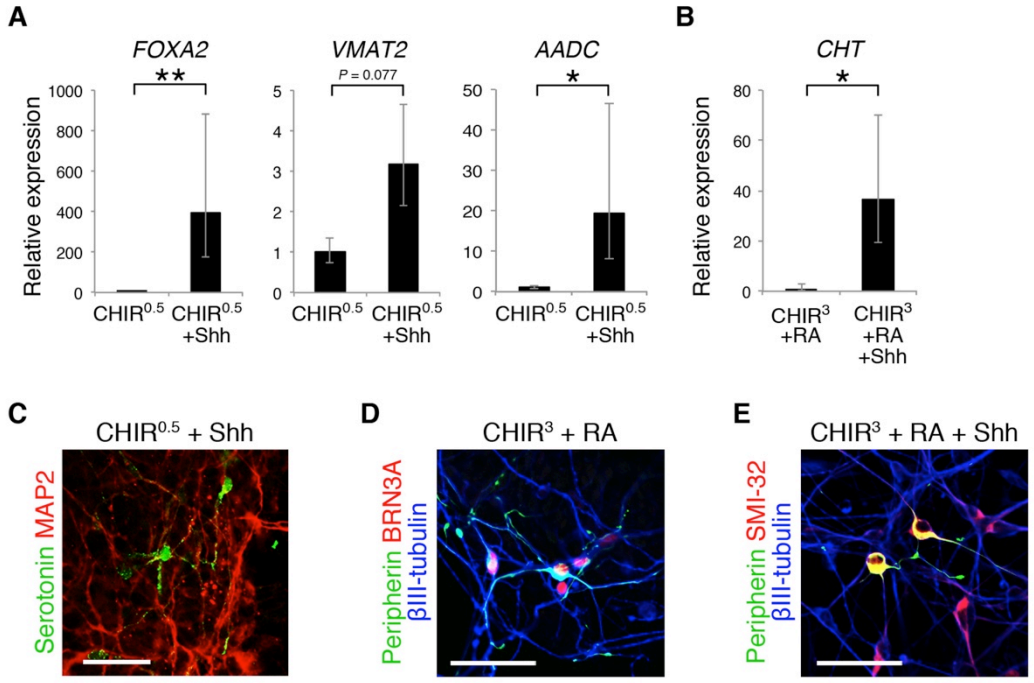

Figure S4. Further characterization of ESC-derived neurons

(A–B) qRT-PCR analysis of neurosphere-derived neurons for the expression of neuronal subtype markers (n = 3 independent experiments; mean ± SEM; *P < 0.05, **P < 0.01; Student's t test).

(C–E) Immunocytochemical analysis of neurosphere-derived neurons for neuronal subtype markers (scale bar = 50 μm).

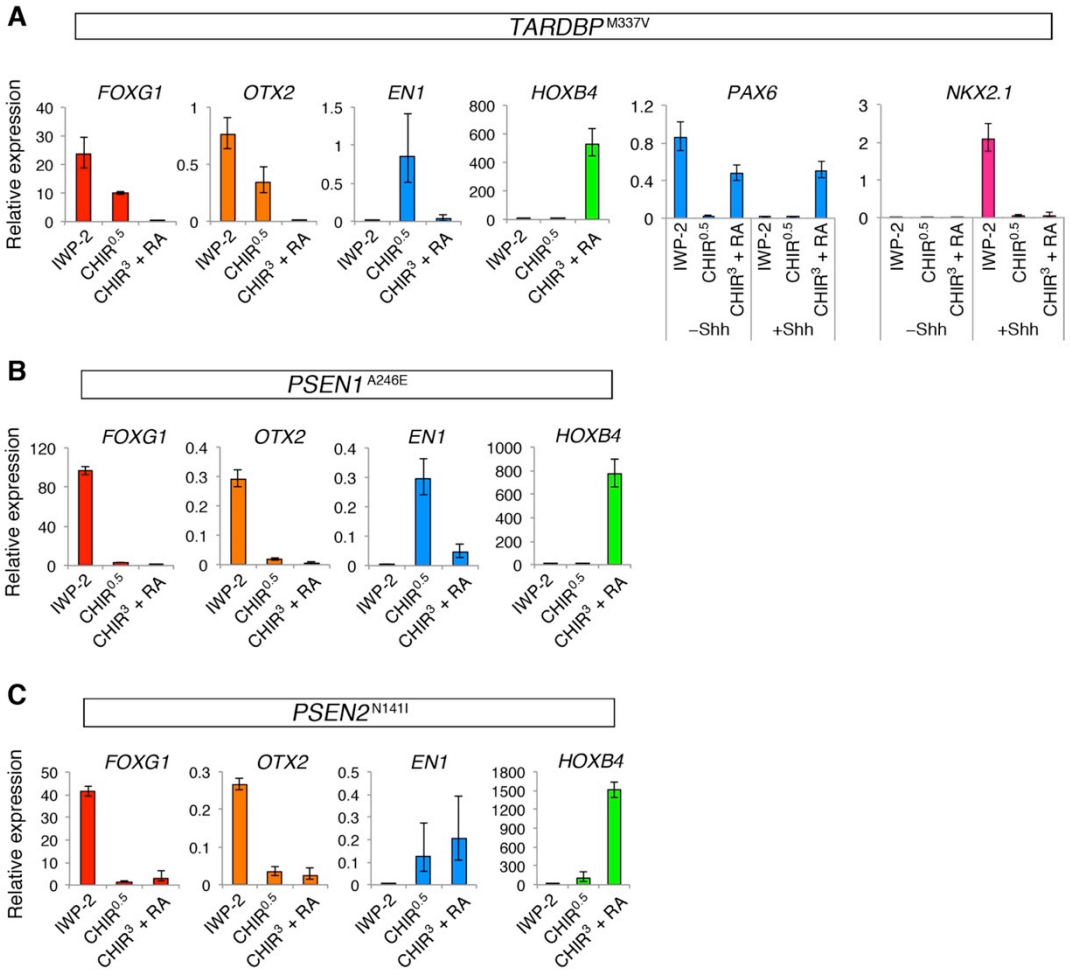

Figure S5. Control of regional identities of disease-specific iPSC-derived neural progenitors

(A) qRT-PCR analysis of *TARDBP* ^{M337V} iPSC-derived neurospheres for regional markers expression relative to the untreated condition of KhES-1 (n = 3 independent experiments; mean ± SEM).

(B) qRT-PCR analysis of *PSEN1* ^{A246E} iPSC-derived neurospheres for regional markers expression relative to the untreated condition of KhES-1 (n = 3 independent experiments; mean ± SEM).

(C) qRT-PCR analysis of *PSEN2* ^{N141I} iPSC-derived neurospheres for regional markers expression relative to the untreated condition of KhES-1 (n = 3 independent experiments; mean ± SEM).

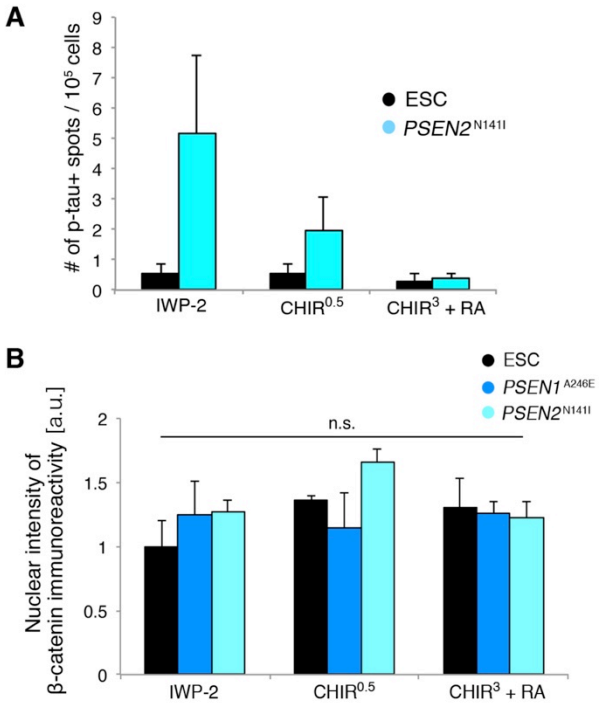

Figure S6. Region-specific phenotypes in the AD iPSC cultures

(A) Quantification of p-tau+ spots (n = 3 independent experiments; mean ± SEM). The data obtained from ESC cultures are same as shown in Fig.5.

(B) Quantification of nuclear intensity of β-catenin immunoreactivity (n = 3 independent experiments; mean ± SEM; n.s., not significant; ANOVA). See also Supplemental Experimental Procedures.

Table S1. Summary of immunocytochemical quantification

	Neurosphere[a]						Neuron[b]	
	FOXG1	OTX1	HOXB4	PAX6	NKX2.1	NKX2.2	TBR1	HB9
IWP-2	41 ± 1	8 ± 2	0 ± 0	81 ± 8	0 ± 0		23 ± 10	
IWP-2 + Shh				1 ± 0	40 ± 19		0 ± 0	
untreated	11 ± 2	61 ± 1	0 ± 0					
CHIR[3]	0 ± 0	0 ± 0	14 ± 4					
CHIR[3] + RA	0 ± 0	0 ± 0	63 ± 7	62 ± 21		1 ± 1		0 ± 0
CHIR[3] + RA + Shh				85 ± 4		20 ± 4		44 ± 3

[a]The frequency of neurospheres containing immunopositive cells is shown as the percentage of total neurospheres (n = 3 independent experiments; mean ± SEM).
[b]The frequency of immunopositive cells is shown as the percentage of MAP2+ neurons (n = 3 independent experiments; mean ± SEM).

Table S2. List of qRT-PCR primers

Gene	Forward	Reverse
AADC	AGGAAGCCCTGGAGAGAGAC	ATTGTCAAAGGAGCAGCATGT
ACTB	TGAAGTGTGACGTGGACATC	GGAGGAGCAATGATCTTGAT
ASCL1	GATGAGTAAGGTGGAGACACTGCG	CCGACGAGTAGGATGAGACCG
CHT	ATCCCAGCCATACTCATT	CAGAAACTGCACCAAGACCA
DLX2	ACGCTCCCTATGGAACCAGTT	TCCGAATTTCAGGCTCAAGGT
EMX1	AGGTGAAGGTGTGGTTCCAG	AGTCATTGGAGGTGACATCG
EMX2	GCTTCTAAGGCTGGAACACG	CCAGCTTCTGCCTTTTGAAC
EN1	CCGCGCACCAGGAAGCTGAA	CAGCGCCAGGCCGTTCTTGA
FOXA2	CCGTTCTCCATCAACAACCT	GGGGTAGTGCATCACCTGTT
FOXG1	CCCGTCAATGACTTCGCAGA	GTCCCGTCGTAAAACTTGGC
GATA3	CAGACCACCACAACCACACTCT	GGATGCCTTCCTTCTTCATAGTCA
HB9	GTCCACCGCGGGCATGATCC	TCTTCACCTGGGTCTCGGTGAGC
HOXB4	ACGTGAGCACGGTAAACCCCAA	ATTCCTTCTCCAGCTCCAAGACCT
HOXC4	TTCACGTTAGCACGGTGAAC	GACTTTGGTGTTGGGGAGTC
LBX1	CGCCAGCAAGACGTTTAAG	CTGCCCAAAGATGGTCATAC
LHX6	GCAGAACAGCTGCTACATCAAGAA	CAGTCGCTGGCGTAGATCTGTC
LHX8	GTGTCATACAGGTGTGGTTTC	GGGTACGTAGGCAGAATAAG
LHX9	GATGCCAAGGACCTCAAGC	CTCGTGCGTTTTGGAACC
LMX1A	GATCCCTTCCGACAGGGTCTC	GGTTTCCCACTCTGGACTGC
NESTIN	TTCCCTCAGCTTTCAGGACCCCAA	AAGGCTGGCACAGGTGTCTCAA
NGN2	CCTGGAAACCATCTCACTTCA	TACCCAAAGCCAAGAAATGC
NKX2.1	AGGGCGGGGCACAGATTGGA	GCTGGCAGAGTGTGCCCAGA
NKX2.2	AAACCATGTCACGCGCTCA	GGCGTTGTACTGCATGTGCT
OTX1	CACTAACTGGCGTGTTTCTGC	GGCGTGGAGCAAAATCG
OTX2	ACAAGTGGCCAATTCACTCC	GAGGTGGACAAGGGATCTGA
PAX6	ACCACACCGGTTTCCTCCTTCACA	TTGCCATGGTGAAGCTGGGCAT
PAX7	CTTCAGTGGGAGGTCAGGTT	CAAACACAGCATCGACGG
PET1	CGGCGGCGATGAGACAGAGCGGCGCCTCC	ACGCGATGCAGCCGGCGTTCGCGCGGTCA
SIX3	ACCGGCCTCACTCCCACACA	CGCTCGGTCCAATGGCCTGG
TBR1	ATGGGCAGATGGTGGTTTTA	GACGGCGATGAACTGAGTCT
TH	TCATCACCTGGTCACCAAGTT	GGTCGCCGTGCCTGTACT
VMAT2	CGGATGTGGCATTTTGTATGG	TTCTTCTTTGGCAGGTGGACTTC

Table S3. List of Antibodies and Dilutions

Protein	Species	Source (cat. #)	Dilution
βIII-tubulin	Mouse	Sigma (T8660)	1:500
β-catenin	Mouse	BD Transduction Laboratories (610154)	1:200
BRN3A	Mouse	Chemicon (MAB1585)	1:500
FOXG1	Rabbit	Abcam (ab18259)	1:500
GFAP	Rat	Invitrogen (13-0300)	1:500
HB9	Mouse	DSHB (81.5C10)	1:250
HOXB4	Rat	DSHB (I12)	1:100
MAP2	Mouse	Sigma (M4403)	1:500
MAP2	Rabbit	Chemicon (AB5622)	1:1000
NKX2.1	Mouse	Invitrogen (18-0221)	1:50
NKX2.2	Mouse	DSHB (74.5A5)	1:100
O4	Mouse	Chemicon (MAB345)	1:4000
OTX1	Mouse	DSHB (5F5)	1:5000
p-tau	Mouse	Innogenetics (90206)	1:500
PAX6	Rabbit	MBL (PD022)	1:200
Peripherin	Rabbit	Chemicon (AB1530)	1:1000
Serotonin	Goat	Immunostar (20079)	1:500
SMI-32	Mouse	Covance (SMI-32P)	1:2500
Synaptotagmin	Mouse	gift from Dr. Makoto Itakura	1:250
TBR1	Rabbit	Abcam (ab31940)	1:200
VAMP2	Rabbit	gift from Dr. Makoto Itakura	1:250

Supplemental Experimental Procedures

Neurosphere formation assay

Neurosphere size was assessed by measuring neurosphere diameters on differentiation day 7 by using the IN Cell Analyzer 1000 System (GE Healthcare Biosciences). Only neurospheres larger than 20 μm in diameter were analyzed.

Calcium imaging

Calcium imaging analyses were performed as described previously (Shimada et al., 2012; Zhou et al., 2014). For calcium dye loading, cells attached on glass coverslips were incubated at 37°C for 20 min with 4 μM Fluo-4 AM (Thermo Fisher Scientific) in imaging solution (117 mM NaCl, 2.5 mM KCl, 2 mM $CaCl_2$, 2 mM $MgSO_4$, 25 mM HEPES and 30 mM D-(+)-glucose), followed by washing for 30 minutes in imaging solution. Coverslips were then transferred into a custom-made field stimulation chamber and continuously perfused at 2 ml/min with imaging solution. Time-lapse image sequences (20× magnification) were acquired at 2 Hz using a Nikon Eclipse microscope (Nikon) equipped with a cooled CCD camera (iXon, Andor Technology). Extracellular field stimulation was performed with two parallel platinum wires at 25 V/cm. Each stimulation was a train of 500 microsecond pulses at 40 Hz for 5 seconds. The fluorescence change over time is defined as $\Delta F/F = (F - F_0)/F_0$, where F = the fluorescence at a given time point and F_0 = the fluorescence at time zero of each cell. To assess changes in calcium signaling in response to perturbation of neuronal activity, 0.2 μM the voltage-gated sodium channel blocker tetrodotoxin (TTX; Alomone Labs) was applied by bath application.

Quantification of nuclear β-catenin intensity

To assess GSK3β activity, the nuclear intensity of β-catenin immunoreactivity was quantified through automated image acquisition and analysis by using an IN Cell Analyzer 6000 System (GE Healthcare Biosciences) based on a protocol modified from Kirkeby and colleagues (Kirkeby et al., 2012).

Supplemental References

Kirkeby, A., Grealish, S., Wolf, D. a, Nelander, J., Wood, J., Lundblad, M., Lindvall, O., and Parmar, M. (2012). Generation of regionally specified neural progenitors and functional neurons from human embryonic stem cells under defined conditions. Cell Rep. *1*, 703–714.

Shimada, H., Okada, Y., Ibata, K., Ebise, H., Ota, S.I., Tomioka, I., Nomura, T., Maeda, T., Kohda, K., Yuzaki, M., et al. (2012). Efficient Derivation of Multipotent Neural Stem/Progenitor Cells from Non-Human Primate Embryonic Stem Cells. PLoS One *7*.

Zhou, Z., Kohda, K., Ibata, K., Kohyama, J., Akamatsu, W., Yuzaki, M., Okano, H.J., Sasaki, E., and Okano, H. (2014). Reprogramming non-human primate somatic cells into functional neuronal cells by defined factors. Mol. Brain *7*, 24.